Available online at www.sciencedirect.com
ScienceDirect
C. R. Physique 10 (2009) 491–503
COMPTES RENDUS PHYSIQUE
http://france.elsevier.com/direct/COMREN/

Theoretical spectroscopy / Spectroscopie théorique

Ab initio absorption spectra of 3-tert-butylcyclohexene

Katalin Gaál-Nagy [a,b,*], Olivia Pulci [a,c], Giovanni Onida [a,b]

[a] *European Theoretical Spectroscopy Facility (ETSF)*
[b] *CNISM-CNR-INFM, and Dipartimento di Fisica dell'Università di Milano, via Celoria 16, 20133 Milano, Italy*
[c] *CNR-INFM and Dipartimento di Fisica dell'Università di Roma "Tor Vergata", Via della Ricerca Scientifica, 00133 Roma, Italy*

Available online 4 December 2008

Abstract

We present an *ab initio* investigation of the optical properties of 3-tert-butylcyclohexene in both its conformers. The optical spectra, here the photoabsorption cross section, have been obtained within density-functional theory at the independent-particle level, and within time-dependent density-functional theory. The optical spectra of the two conformers show small but visible differences, hence suggesting that optical absorption experiments can discriminate among the two molecular geometries. ***To cite this article: K. Gaál-Nagy et al., C. R. Physique 10 (2009).***

Résumé

Spectres d'absorption ab initio du 3-tert-butylcyclohexène. Nous présentons une étude ab-initio des propriétés optiques de la molécule 3-tert-butylcyclohexène, dans ses deux conformères. Les spectres optiques, assimilés à la section efficace de photo-absorption, sont calculés en théorie de la fonctionnelle densité au niveau des particules indépendantes, et dans le cadre de la théorie de la fonctionnelle de densité dépendante du temps (TDDFT). Les spectres des deux conformères montrent des différences, petites mais visibles, et suggèrent la possibilité d'utiliser la spectroscopie optique pour distinguer parmi les deux structures moléculaires. ***Pour citer cet article : K. Gaál-Nagy et al., C. R. Physique 10 (2009).***

Keywords: Absorption spectra; 3-tert-butylcyclohexene

Mots-clés : Spectres d'absorption ; 3-tert-butylcyclohexène

1. Introduction

The study of chiral molecules and associated phenomena is a very active area. Chiral carbon compounds are of interest in pharmacy and in biological processes for many years. In particular, the conformationally flexible alkene 3-tert-butylcyclohexene has been studied in the past, [1–3] since it is, e.g., a detectable end product after a hydrolysis in the rabbit liver [4]. It plays also a major role in the preparation of epoxides as a basis for the formation of halohydrins [1]. Depending on the conformation of 3-tert-butylcyclohexene, various reactions can occur. Often, X-ray refraction data give insufficient information to describe the molecule. Therefore, optical measurements, which are fast

* Corresponding author.
E-mail address: katalin.gaal-nagy@physik.uni-regensburg.de (K. Gaál-Nagy).

1631-0705/$ – see front matter
doi:10.1016/j.crhy.2008.08.002

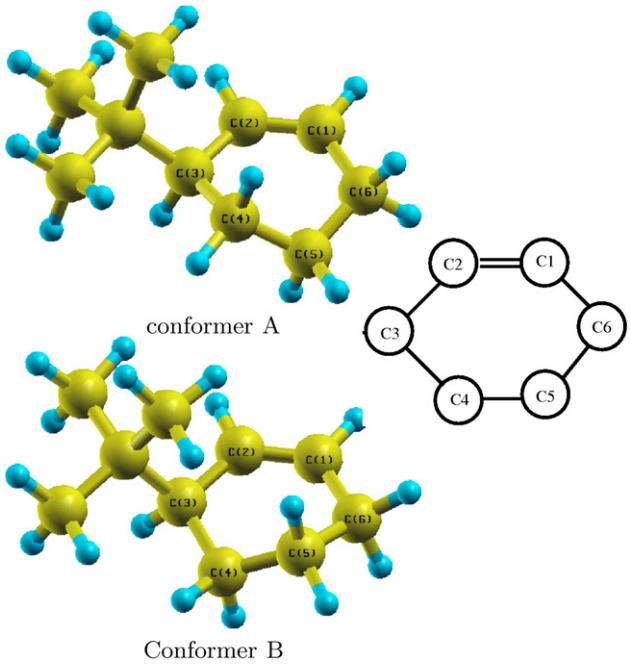

Fig. 1. (color online) Atomic structure of conformer A (upper panel) and conformer B (lower panel) of 3-tert-butylcyclohexene. Carbon atoms are displayed as large (yellow) spheres and hydrogen atoms as small (blue) ones.

and simple, can give the required additional information, provided that reliable calculations of the optical spectra are available.

3-tert-butylcyclohexene (C10H18) is the only 3-alkylcyclohexene with optical activity [3]. Moreover, it is the one with the most extended alkyl group. The tert-butyl group can also enhance the chemical reactivity of the molecule [5]. The atomic structure of the two existing conformers are shown in Fig. 1. They consist of 10 carbon (C) and 18 hydrogen (H) atoms. According to the name, it is built up from a hexene ring (carbon atoms C1 to C6, counted anticlockwise from the double bond between C1 and C2) and a tert-butyl group, which is attached at the third carbon atom (C3) from the double bond of the cyclohexene, resulting in a 3-tert-butyl compound.

Experimentally, 3-tert-butylcyclohexene can be produced by dehydrotosylation of the tosylate of cis-3-tert-butylcyclohexanol [6]. A possible confirmation of the existence of 3-tert-butylcyclohexene as a reaction product is the measurement of its optical rotation. The optical rotation was detected not only for the commonly used sodium D line, but also for various wavelengths of light by Bellucci et al. [6] and by Sadozai et al. [3] However, an ab-initio calculation of the optical rotation has lead to a qualitative agreement but with the wrong sign [7]. The molecule is conformationally flexible and both conformers are close in energy. This might be a source of the discrepancy. Nevertheless, it is also speculated that the absolute configuration of the molecule is not assigned correctly.

A complementary investigation of the optical properties of 3-tert-butylcyclohexene might be given by the measurement of its absorption spectra. It would be interesting to know if the optical properties of the two conformers are significantly different. Ab-initio calculations can give reliable results for optical properties. The quality of the calculations can vary from the independent-particle approximation (IPA) within the density-functional theory (DFT) to many-body perturbation theory and to the time-dependent density-functional theory (TDDFT) [8,9]. In this article, we focus on the DFT based approximations, the DFT-IPA and the TDDFT. The DFT-IPA is a tool which can be easily applied: the calculations are not computationally heavy and the resulting spectra can be analyzed with respect to the origin of the peaks in an intuitive way. However, being DFT a ground state theory, the quantitative agreement of the spectra with experimental results is often not very good. TDDFT, on the other hand, is, in principle, able to take into account the excited state properties of the system in an exact way. It is a more elaborated theory giving good results compared with experimental spectra, but the computations are more demanding. The main scope of this work is to figure out if the two conformers can be distinguished by optical absorption measurements. This could foster experi-

mental investigations which are still missing but which are necessary in order to clarify the absolute configuration of 3-tert-butylcyclohexene.

This article is organized as following: First, we give an overview of the theoretical approaches employed in our calculations (Section 2). Second, we present the results for the ground-state properties of 3-tert-butylcyclohexene in Section 3 and its optical properties in Section 4. Finally, we draw our conclusions.

2. Theoretical and computational background

2.1. Ground state

We have performed ab initio total energy calculations within the density-functional theory framework [10] (DFT) applying the local-density approximation [11,12] (LDA) and the generalized-gradient approximation (GGA) using the Becke–Lee–Yang–Parr [13,14] (BLYP) functional. We have employed two different implementations of the DFT for our calculations: QUANTUM-ESPRESSO [15] and OCTOPUS [16]. Both codes are based on a self-consistent solution of the Kohn-Sham equations, [17]; in QUANTUM-ESPRESSO the eigenfunctions are expanded in plane waves and in OCTOPUS the eigenfunctions are represented by their discretised values on an uniform spatial grid. In order to avoid an explicit description of the internal (core) electrons, we have used norm-conserving pseudopotentials in the Troullier–Martins [18] and in the von Barth [19,20] style in both codes, respectively.

QUANTUM-ESPRESSO bases on a periodic-cell approach. The study of an isolated molecule using periodic-boundary conditions requires the use of a supercell with the molecule in the center and which is empty otherwise. Only the Γ point is necessary to sample the reciprocal space due to the 0-dimensionality of the system. Therefore, the convergence of the ground state depends on the kinetic-energy cutoff which determines the number of plane waves in the expansion and on the size of the supercell.

OCTOPUS bases on a real-space approach [21,22]. Due to the discretization of the wavefunctions in real space, the two parameters to converge are the spacing of the real-space grid and the size of the simulation box. Here, we have performed LDA calculations only.

2.2. Optical properties

In a first step, the optical spectra, in particular the dynamical polarizability $\alpha(\omega)$ as a function of the energy ω, has been calculated in the independent particle approach (IPA) [23]. The probability $P_{v\mathbf{k},c\mathbf{k}}$ of the transitions between valence (v) and conduction (c) states with electronic eigenenergies $E_{c\mathbf{k}}$ and $E_{v\mathbf{k}}$ at a given point $\mathbf{k}$ in the reciprocal space can be calculated as the diagonal elements of the velocity operator [24]. Working within the IPA, local-field, self-energy, and excitonic effects are neglected. The use of a supercell implies the use of the Γ point only, so sum over $\mathbf{k}$ points can be neglected. Thus, the imaginary part of the dielectric function $\mathrm{Im}[\varepsilon]$ writes as

$$\mathrm{Im}\big[\varepsilon_\nu(\omega)\big] = \frac{8\pi^2 e^2}{m^2\omega^2} \sum_{v,c} \big|P^\nu_{v,c}\big|^2 \times \delta(E_c - E_v - \hbar\omega) \tag{1}$$

In this approximation, only the matrix elements $P^\nu_{v,c}$ ($\nu = x, y, z$)) and the electronic eigenenergies are required, which can be easily obtained within the DFT using QUANTUM-ESPRESSO. The dynamic polarizability α_ν ($\nu = x, y, z$) is directly connected with the dielectric function ε_ν by $\varepsilon_\nu = (1 + 4\pi\alpha_\nu)/V$.

Within TDDFT there are two possibilities to calculate the absorption spectra: they can be calculated based on the real-time evolution of the ground-state density [25,26] or based on the time-dependent density-functional linear response theory in configuration space, as proposed by Casida [27–31].

In the first case, the evolution of the density $n(\mathbf{r}, t)$ after a small perturbation can be written as

$$n(\mathbf{r}, t) = n_{\mathrm{GS}}(\mathbf{r}, t) + \delta n(\mathbf{r}, t)$$

where $n_{\mathrm{GS}}(\mathbf{r}, t)$ is the ground state density. The susceptibility χ is the linear response of the ground state to a small variation $\delta\upsilon_{\mathrm{ext}}$of the external potential υ_{ext}, and thus

$$\delta n(\mathbf{r}, \omega) = \int \mathrm{d}\mathbf{r}'\chi(\mathbf{r}, \mathbf{r}', \omega)\delta\upsilon_{\mathrm{ext}}$$

Assuming $\delta v_{\text{ext}} = -k_0 r_\nu \delta(t)$, the dynamic polarizability $\alpha_\nu(\nu = x, y, z)$ can be calculated as [32]

$$\begin{aligned}\alpha_\nu(\omega) &= -\frac{1}{k_0}\int \mathrm{d}\mathbf{r}\, r_\nu\, \delta n(\mathbf{r},\omega) \\ &= -\int \mathrm{d}\mathbf{r}\int \mathrm{d}\mathbf{r}'\, r_\nu\, \chi(\mathbf{r},\mathbf{r}',\omega) r'_\nu\end{aligned}$$

For this procedure we have applied the OCTOPUS package.

Within the formalism of Casida, the mixing of states is included by a coupling matrix. This scheme is implemented in OCTOPUS, too. Even if this formalism can be less accurate than the real-time evolution since a linearization of the response of the exchange-correlation functional is applied, it is more accurate than the DFT-IPA. Furthermore, it allows an interpretation of the spectral features in a similar way as for the DFT-IPA spectra. Within the real-time evolution method, the optical properties are calculated from the response of the KS ground-state density only, while the Casida formalism requires the knowledge of the unoccupied states. The mean dynamical polarizability $\bar{\alpha}(\omega) = \frac{1}{3}(\alpha_x + \alpha_y + \alpha_z)$ is obtained using the sum over states theorem

$$\alpha_\nu(\omega) = \sum_I \frac{f_I^\nu}{\omega_I^2 - \omega^2} \tag{2}$$

where the excitation energies ω_I are the eigenvalues of

$$\Omega F_I = \omega_I F_I \tag{3}$$

and the oscillator strength f_I are connected to the eigenvectors F_I. The matrix Ω is derived from an expression containing the KS eigenvalues of occupied and empty states, the occupation numbers of the corresponding states, and a coupling matrix, which incorporates collective electronic excitations, i.e., the mixing of the eigenstates of the system.

The imaginary part of the polarizability function $\bar{\alpha}$ is directly related to the absorption of the media, since the photo-absorption cross section $\sigma(\omega)$ can be written as [9]

$$\sigma(\omega) = \frac{4\pi\omega}{c_0}\,\mathrm{Im}\big[\bar{\alpha}(\omega)\big] \tag{4}$$

where c_0 is the velocity of light.

2.3. Convergence tests

Using a plane-wave approach with periodic boundary conditions for a molecule, the two convergence parameters to check are the kinetic-energy cutoff E_{cut} and the size of the supercell. To address the non-cubic character of 3-tert-butylcyclohexene, we have chosen an orthorhombic supercell with ratios $b/a = 1.1$ and $c/a = 0.6$ (a, b, and c are the lattice parameters of the orthorhombic supercell), which reflect the extension of the molecule. Hence, the size of the supercell is determined by the lattice parameter a only. Both the choice of E_{cut} and a influence the number of plane waves used in the calculation. Due to the similarity of the two conformers, we have performed the convergence tests exclusively for conformer A. We considered LDA and GGA separately; however, the results for GGA do not differ significantly from those using LDA.

Looking forward to the optical properties, which depend strongly on the convergence of the empty states, we inspected, besides the total energy, also the HOMO-LUMO gap as a function of the supercell lattice parameter a and E_{cut}. It turned out that the total energy is less sensitive to a variation of a than to a variation of E_{cut}. On the contrary the gap is more sensitive to a variation of a than a variation of E_{cut}. A choice of $E_{\text{cut}} = 60$ Ry and $a = 50$ a_B yields a convergence of the total energy better than 1 eV and of the gap better than 10 meV.

Also for OCTOPUS we inspected the total energy and the gap, here as a function of the radius of the simulation box, and the grid spacing. Careful tests yield the converged values, a spacing of 0.15 Å and a radius of 5.0 Å. With these values, the total energy is converged up to 0.1 eV and the gap up to 40 meV.

Table 1
Calculated dihedral angles (in degrees) using the plane-wave (1) and the real-space (2) approach in comparison with theoretical reference data of McCann and Stephens [7]. For the assignment of the carbon atoms see Fig. 1

Conformer A	LDA (1)	GGA (1)	LDA (2)	Ref. [7]
C1C2C3C4	13.086	12.388	13.212	13.04
C2C3C4C5	−44.782	−43.284	−44.248	−43.65
C3C4C5C6	62.491	61.562	61.728	61.63
C4C5C6C1	−44.493	−45.003	−44.060	−44.82
C5C6C1C2	12.905	14.350	12.857	14.39
C6C1C2C3	3.121	2.276	2.771	1.74
Conformer B	LDA (1)	GGA (1)	LDA (2)	Ref. [7]
C1C2C3C4	−8.181	−9.385	−9.011	−7.66
C2C3C4C5	38.865	39.057	39.565	37.16
C3C4C5C6	−59.156	−57.489	−59.629	−57.28
C4C5C6C1	45.654	43.196	45.571	44.64
C5C6C1C2	−16.434	−15.087	−16.549	−16.58
C6C1C2C3	−2.951	−2.433	−2.364	−2.49

3. Ground-state properties

With the convergence parameters above we have relaxed the atomic structure of conformer A and B for LDA and GGA separately. According to the length of the atomic bonds, the two conformers are very similar (see also Fig. 1). We have found that the double-bond distance (C1–C2) is 1.33 Å (1.34 Å) for conformer A (B) in both LDA and GGA. The distance between simple-bonded carbon atoms is 1.51 Å (1.54 Å) using LDA (GGA) for both conformers. The variation of the bondlength using different approximations for the exchange-correlation functional shows the standard slight underestimation of bondlength within LDA. The bonds close to the double bond, C1–C6 and C2–C3, are slightly shorter than the other C–C bonds. The values obtained here are all in the range of bondlength of carbon compounds. Also the C–H bondlength of 1.1 Å is in agreement with observed values.

The main difference between the two conformers is due to their dihedral angles, which are summarized in Table 1 together with available reference data. Inspecting the values one sees that the buckling of conformer A is in the opposite direction than the one of conformer B, whereas the absolute values of the angles is quite similar. Considering reference data, the agreement between our results and those of McCann and Stephens [7] is very good. Note that an addition of, e.g., a 4-cyano or a 4-carboxy substituent to the cyclohexene ring can diminish the buckling [2].

Concerning the total energy of the two conformers it turns out that conformer A is about 5 mRy (65 meV LDA, 68 meV GGA) more stable than conformer B using the plane-wave approach. In the real-space method the energy difference is very similar, 73 meV, showing the same relative stability of the two conformers.

4. Absorption spectra

We have calculated the optical spectra using the DFT-IPA and the TDDFT. Here we want to investigate the differences between the two conformers of 3-tert-butylcyclohexene in $\sigma(\omega)$. Even if TDDFT calculations give more reliable results than the simple DFT-IPA approximation, [9] the independent-particle spectra can give in a very easy way informations about transitions responsible for spectral features. Sometimes, the DFT-IPA calculation of the spectra yields already reasonable results. Thus, a qualitative agreement between TDDFT and DFT-IPA spectra is often enough to transfer the interpretations found for the DFT-IPA results to the TDDFT ones. Here we have performed TDDFT calculations using the Casida formalism as well as the real-time evolution of the density. The latter one is computational demanding and thus we have focused on the Casida results, which we have analyzed in the same manner as the DFT-IPA spectra.

In a first step we have investigated $\sigma(\omega)$ within the DFT-IPA method, where we analyzed the spectral features in detail (Section 4.1). Besides, variations in the spectra with respect to the approximations of the exchange-correlation potential (LDA and GGA) have been discussed. In a next step we have performed TDDFT spectra using the Casida formalism (Section 4.2), which we have compared to the DFT-IPA ones. For the Casida spectra we analyzed the decomposition of $\sigma(\omega)$ with respect to anisotropy effects (Section 4.3). In order to check differences in the TDDFT

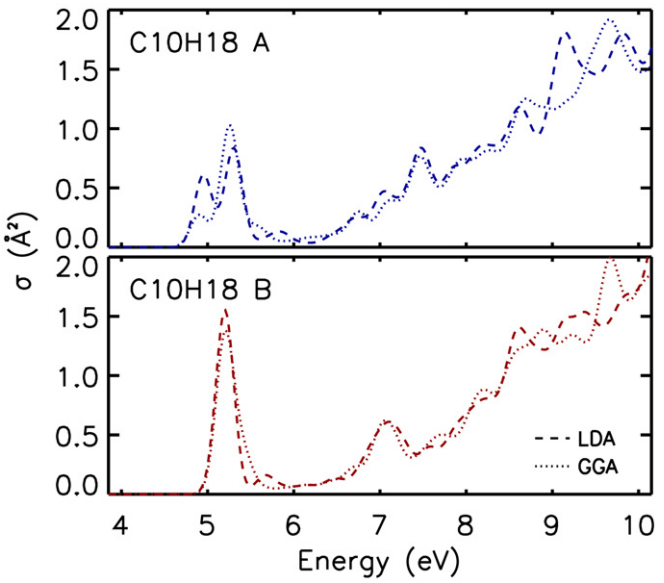

Fig. 2. Comparison of the photo-absorption cross section within DFT-IPA for conformer A (upper panel) and conformer B (lower panel) using the LDA (dashed) and the GGA (dotted) approximation. An average over the three directions has been taken.

results based on the Casida formalism and the real-time evolution of the density, we have calculated also the spectra using the latter method, however, only at low convergence (Section 4.4). Finally, we discuss the value of the optical gap in comparison with available experimental data (Section 4.5).

4.1. Spectra within DFT-IPA

For the calculation of Eq. (1) we have been reinvestigating the convergence with respect to E_{cut} and a, in order to reduce the number of plane waves used in the calculation. Within LDA, the choice of $a = 38$ a_B yields a converged spectra up to 7.5 eV, where the main peaks are still reproduced also for higher energies, and $E_{\text{cut}} = 45$ Ry is sufficient to obtain reliable results in this energy range. Similarly, the parameters using GGA are $E_{\text{cut}} = 45$ Ry and $a = 42$ a_B.

The resulting spectra of the photo-absorption cross section for conformer A and B and with LDA and GGA are presented in Fig. 2 where we applied a Gaussian convolution with a width of 0.1 eV in order to smooth the spectra. In the low-energy range, a double peak is visible for conformer A and a single peak for conformer B, which are reproduced within both LDA and GGA. Thus, the two conformers seem to be clearly distinguishable. Whereas for conformer B the difference between LDA and GGA is negligible, the approximation for the exchange-correlation functional affects the height of the peaks of conformer A. The use of various exchange-correlation functionals leads to slightly different bondlengths. Nevertheless, these differences are rather small (see Section 3), whereas the charge density shows larger variations. Thus, we conclude that the differences are mainly due to the use of different exchange-correlation functionals rather than due to the difference in the atomic positions using LDA and GGA in the groundstate relaxation.

In the following, we analyze the spectra by inspecting the responsible transitions and the location of the charge densities of the corresponding states (see Fig. 3). Common for both conformers and for LDA and GGA, the optical spectra up to ≈ 6 eV are exclusively determined by transitions from the HOMO (state 29), which is strongly localized at the C atoms forming the double bond, to various empty states. On the contrary, transitions from the HOMO-1 (state 28) play a role only at higher energies due to the energy difference between the HOMO and the HOMO-1 of ≈ 1 eV. However, also at higher energies the transition probability from the HOMO-1 remains small, because the localization of its charge along the C–H bonds close to the C=C bond and along various other C–C bonds, whereas the low-energy empty states are localized around C=C.

The first transition is at ≈ 5 eV. The double-peak structure of conformer A comes from transitions between the HOMO and the LUMO (state 30) and the LUMO+1 (state 31). For conformer A, both transitions show a significant

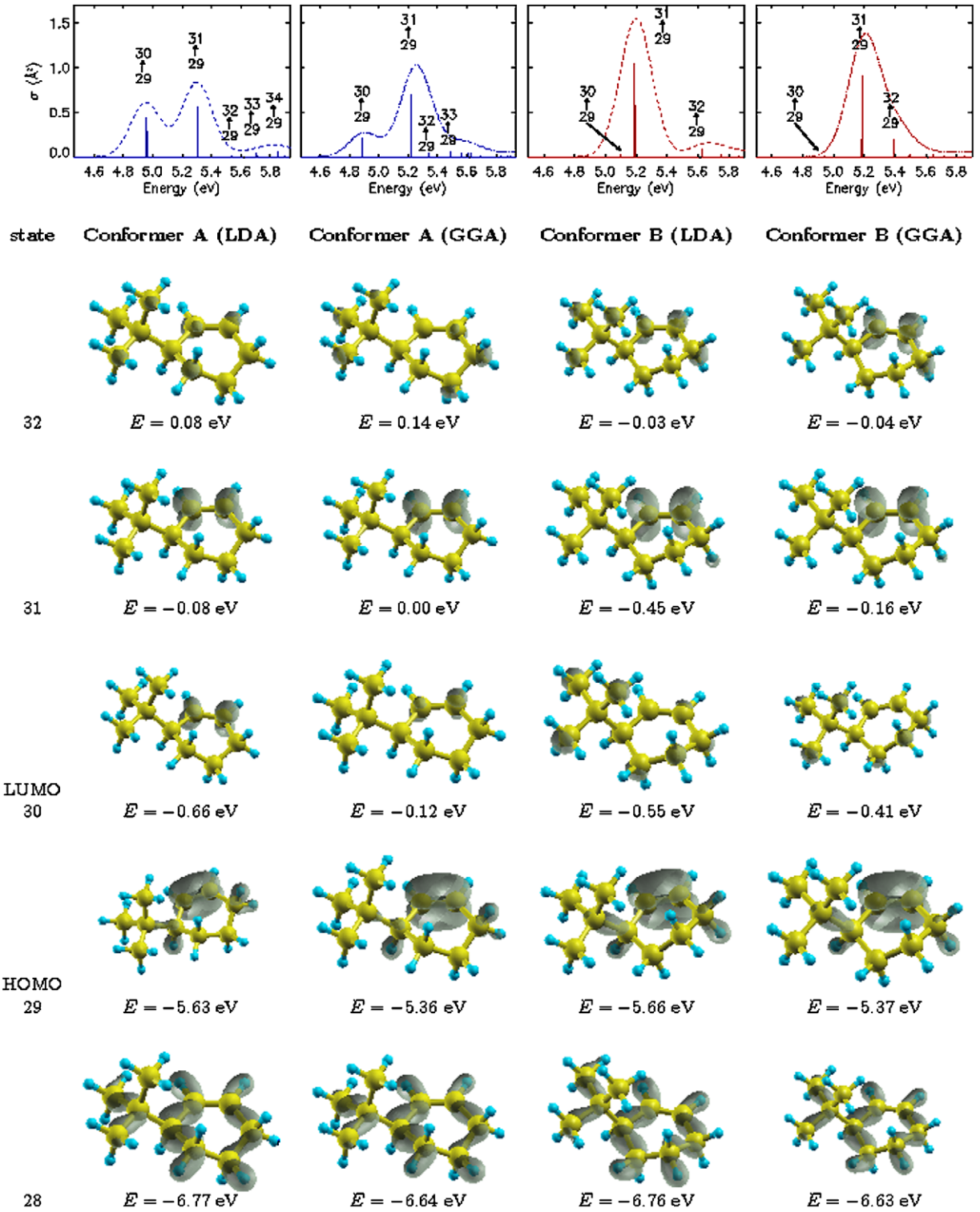

Fig. 3. Low energy range of the spectra shown in Fig. 2, with indication of the responsible transitions (upper panel). Here, state 29 corresponds to the HOMO and 30 to the LUMO. In the lower panel, the charge densities of the important states, labeled by their Kohn–Sham energies (below) and by the state number (left side) is drawn. The leftmost columns refer to conformer A (within LDA and GGA), and the rightmost ones to conformer B (LDA and GGA).

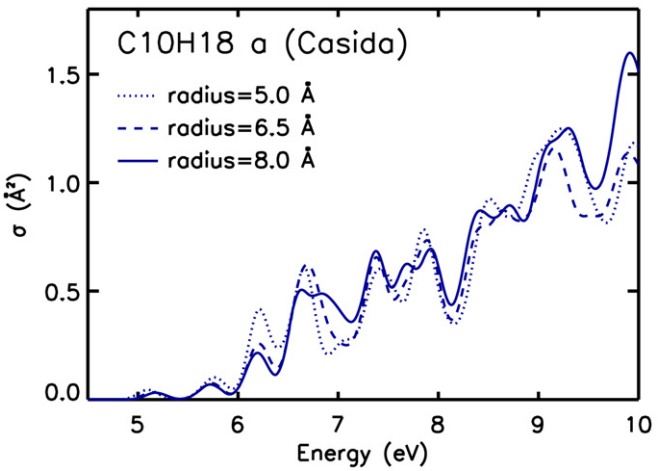

Fig. 4. TDDFT Casida spectra for conformer A using a radius of 5 Å where we have applied an energy shift of 0.2 eV (dotted), a radius of 6.5 Å (dashed) with an energy shift of 0.05 eV, and using a radius of 8 Å (solid).

contribution, while for conformer B the HOMO-LUMO transition nearly vanishes. This is due to the fact that less charge of the LUMO is localized close to the carbon double bond for conformer B than for conformer A. Similar considerations can be done for the transition $29 \rightarrow 32$. Here, for conformer B, more charge is localized at C=C than for conformer A yielding a higher peak for conformer B than for conformer A.

The third (second) peak in the spectra of conformer A (B) is due to the HOMO to LUMO+2 (state 32) transition. Because the eigenenergy of state 32 does not show the same energy shift as the HOMO comparing LDA and GGA, the transition appears only as a shoulder within the GGA calculation. This gives also a hint to the numerical resolution of our calculation.

The next clear spectral structure is a peak at $\approx$7.2 eV for conformer B, which is hidden in the background of other transitions for conformer A. This peak consists mainly of the transitions $25 \rightarrow 30$, $24 \rightarrow 30$, and $27 \rightarrow 32$. For conformer B, the probabilities of these transitions are large compared to neighboring transitions, whereas for conformer A all transitions in this range are in the same order of magnitude.

Last, we want to inspect the charge density in detail. The double bond in cyclohexene is built up from a σ and a π bond. This π bond is clearly visible from the charge density of the HOMO (state 29). The corresponding σ bond corresponds to a low-energy occupied state, which is not drawn here. Nevertheless, the charge density of the HOMO-1 has a σ bond character for the bonds C2–C3, C3–C4, C5–C6, and C6–C1 (including the C–C bonds next to C=C), and various C–H bonds. The empty states have a mixed character, and their charge distribution differs between the conformers.

Since the results using the LDA and the GGA are very similar, we restrict ourselves to the LDA in the following.

4.2. TDDFT spectra using the Casida formalism

The spectra based on the Casida formalism have been calculated using the OCTOPUS code. Since the spectra also incorporate the unoccupied states, we have performed convergence tests with respect to the number of empty states. For 100 states in total the spectra are converged up to 10 eV. In a next step we have investigated the variation of the energies of the empty states with respect to the two parameters, the grid spacing determining the discretization of the wave functions in real space and the radius determining the simulation box. The differences in the eigenenergies using various grids close to the ground-state value of 0.15 Å is less than 0.01 eV. Therefore, the value of 0.15 Å already chosen for the ground state is still valid. The convergence with respect to the radius is much slower. A test calculation of the spectra comparing the results using a radius of 5 Å, 6.5 Å, and 8 Å has demonstrated (see Fig. 4), that the spectra differ mainly in an energy shift of 0.2 eV using radii of 5 Å and 8 Å (an energy shift of 0.05 eV using radii of 6.5 Å and 8 Å) whereas the main spectral features are reproduced. Therefore, the choice of a radius of 8 Å is sufficient.

Comparing the Casida spectra for the two conformers (see Fig. 5) with the DFT-IPA ones there are some large differences in the low-energy range, whereas at higher energies (larger than 7 eV) the difference is quite small. Es-

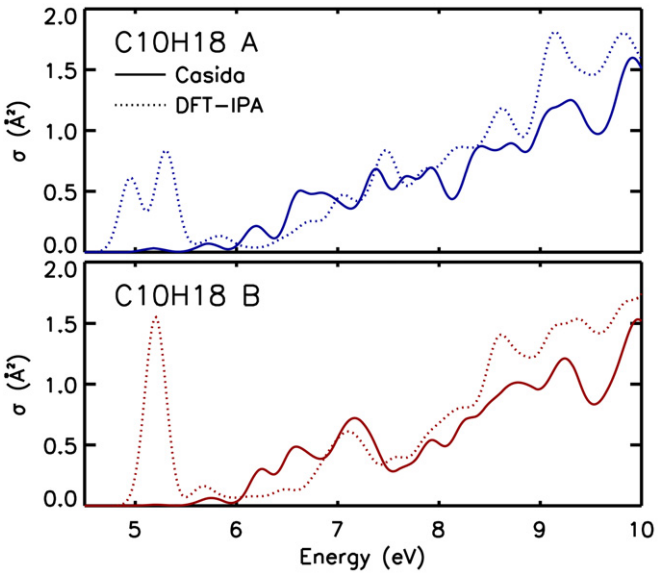

Fig. 5. Comparison of the photo-absorption cross section σ within the TDDFT using the Casida formalism (solid line) and within the DFT-IPA using LDA (dotted line) for conformer A (upper panel) and conformer B (lower panel).

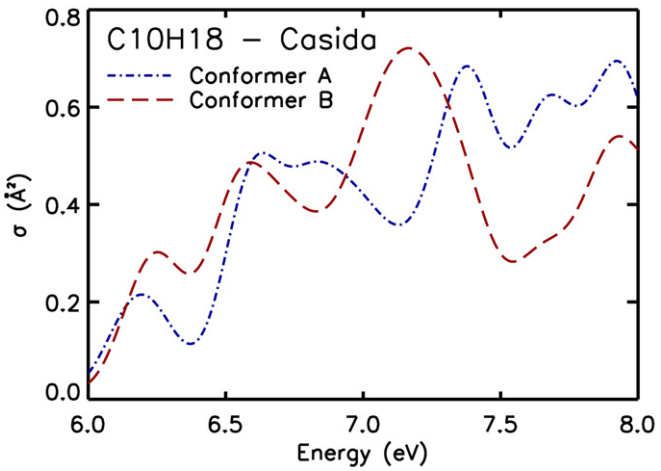

Fig. 6. Comparison of the photo-absorption cross section σ within the TDDFT using the Casida formalism of conformer A (dash-dotted line) and conformer B (dashed line) for the 6–8 eV energy range.

pecially the large double peak for conformer A and the single peak for conformer B disappear in the TDDFT Casida spectra. These features in the DFT-IPA spectra have been the main peaks to distinguish the two conformers. However, the two conformers can still be distinguished inspecting the absorption spectra because of the difference in the energy range between 7 and 8 eV (see Fig. 6), where for conformer A there is first a valley at 7.15 eV and then some peaks between 7.3 and 7.8 eV and conformer B there is a peak at 7.15 eV and a valley between 7.3 and 7.8 eV.

In order to find out the origin of the TDDFT spectral features, we have analyzed the spectra with respect to the responsible transitions in the same manner as for the DFT-IPA spectra. However, due to the mixing of states, often more transitions contribute to a peak at a single energy in the Casida spectra, whereas in the DFT-IPA spectra each sharp peak corresponds mostly to only one transition.

For conformer A, the first tiny peak at 5.2 eV in the Casida spectra is exclusively due to the transitions from the HOMO to the LUMO and the LUMO+1. This means that this peak is split in the DFT-IPA spectra (see also Fig. 3) due to the missing mixing of states. The oscillator strength is overestimated in the DFT-IPA spectra, too. The shift of

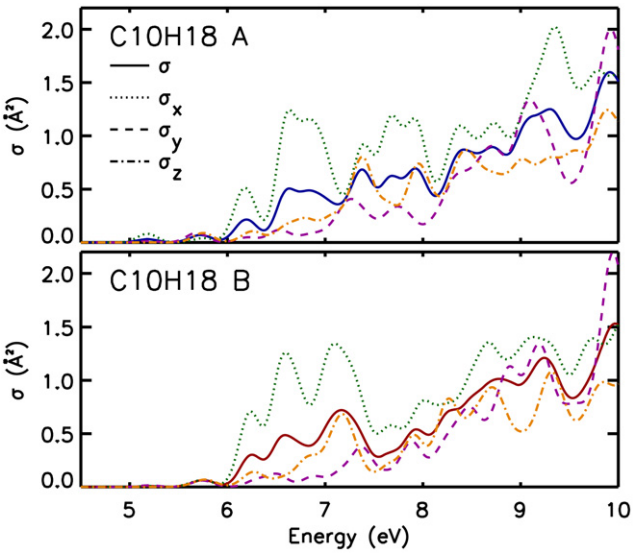

Fig. 7. Decomposition of σ calculated within the Casida formalism (solid line) into the components σ_x (dotted line), σ_y (dashed line), σ_z (dash-dotted line) for conformer A (upper panel) and conformer B (lower panel).

oscillator strength to higher energies is due to the local-field effects which are neglected in the DFT-IPA description. A similar peak is found at 5.2 eV for conformer B, however, at a much less extent. Also for conformer B the peak comes exclusively from transitions between state 29 and the states 30 and 31. As seen in Fig. 3, the broad peak in the DFT-IPA spectra consists of two peaks. Therefore, the difference in the Casida and DFT-IPA spectra for conformer B has the same explanation as for conformer A. The next tiny spectra feature at 5.6 eV in the Casida spectra is due to three peaks (as in the DFT-IPA case) consisting mainly of transitions $29 \rightarrow 32$, $29 \rightarrow 33$, $29 \rightarrow 34$, where also other transitions are involved due to the mixing. For the following peaks much more transitions are involved resulting also in a larger oscillator strength in the Casida spectra than in the DFT-IPA ones. Nevertheless, the main transitions in the Casida case are similar to the DFT-IPA picture. To summarize, the missing mixing in the DFT-IPA spectra yields in some cases a split of peaks and the oscillator strength is overestimated in the low-energy range and underestimated in the medium-energy range. For both approaches, an analysis of the transitions responsible for spectral features gives similar results. However, a direct transfer of the DFT-IPA interpretation to the TDDFT spectra remains difficult, since it is not predictable which peaks might be split in the DFT-IPA case.

4.3. Discussion of anisotropy effects

Since we have now accurate absorption spectra, we want to analyze them also with respect to anisotropy effects. For that purpose we have drawn the decomposition of σ in σ_x, σ_y, and σ_z in Fig. 7 for the spectra calculated within the Casida formalism. The Cartesian axis have been chosen as follows: the x axis is along the direction of the largest extent of the molecule, meaning the direction where the tert-butyl group is attached at the cyclohexene ring. It is more or less along the line of the C3–C bond. However, due to the buckling of the molecule, there is not a pair of atoms exactly placed on the x axis. The y axis is placed perpendicular to x in the "plane" of the cyclohexene ring and the z axis, perpendicular to the x–y plane, is more or less along the C3–H bond.

As shown in Fig. 7, the largest contribution to σ comes from σ_x which gives the absorption spectra the characteristic shape. But σ_z also gives in some parts of the energy range significant contributions, whereas σ_y is small. Considering conformer A (upper panel of Fig. 7), the first peak at 5.2 eV has a large x component, whereas the y and the z components are nearly vanishing. This peak had been found due to transitions $29 \rightarrow 30$ and $29 \rightarrow 31$. From the charge-density analysis in DFT-IPA (see Fig. 3), state 29 was located along the C1–C2 double bond and in parts at the H atoms attached at atom C3 and C6, whereas the states 30 and 31 are both mainly located at the atoms C1 and C2. This means that these transitions occur mainly in the x direction yielding the large σ_x contribution.

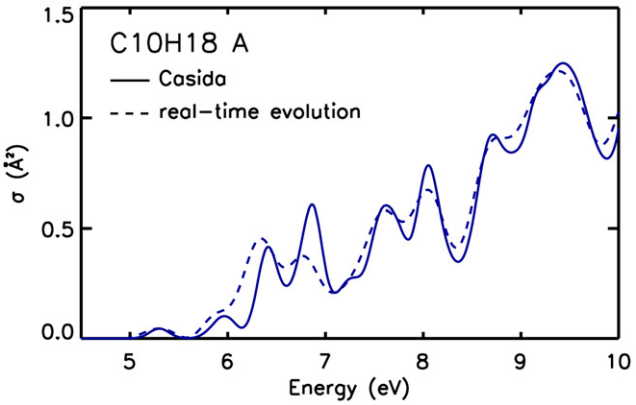

Fig. 8. Comparison of the TDDFT spectra using the Casida formalism (solid line) and the real-time evolution (dashed line) for conformer A. Note: the calculations have been performed using a radius of 5 Å.

Note that the main difference in the absorption spectra of conformer A and conformer B, the valley-peak structure for conformer A and the peak-valley one for conformer B between 7 and 8 eV, is strongly influenced by σ_z. This can be explained by the main difference of the molecules: the cyclohexene ring is oppositely buckled for the two conformers and this buckling occurs in z direction according to our choice of the Cartesian directions.

From this analysis of σ it is clear that the difference between the two conformers is more accessible looking at the x, y, and z components than from the average. Thus, anisotropy spectroscopy on ordered molecular samples would be an experimental tool which would enhance the possibility of distinguishing the two conformers in a better way than standard absorption or transmission experiments. For example, in reflectance-anisotropy experiments of 3-tert-butylcyclohexene molecules attached on a substrate in an ordered way it would be possible to study the anisotropy visible in Fig. 7.

4.4. Spectra within real-time density evolution TDDFT

We have also calculated TDDFT spectra using the real-time density evolution method as described in Section 2. Even though the spectra are based on the time evolution of the ground-state density, the convergence parameters (radius, grid spacing) which guaranteed convergence for the ground state, should also be reinspected. In particular, a too small size of the simulation box will restrict the evolution of the density and can therefore yield erroneous results. In addition to the ground-state convergence parameters, the quality of the spectra depends also on the time step Δt and the evolution time.

Since the calculations based on the density evolution are computationally very demanding, we wanted to determine first if the spectra based on the real-time density evolution method differ much from the Casida ones, and with this, if we will get additional information out of the new spectra. Thus, we have performed real-time evolution calculations using the ground-state convergence parameters (a radius of 5 Å and a grid spacing of 0.15 Å) keeping in mind that the results are not fully converged. For this calculation we have used a time step of 0.012 a.u. and the density was able to evolve for 18 a.u. (1 a.u. $= 2.4 \times 10^{-2}$ fs). The resulting spectra together with the Casida ones using the same radius and the same grid spacing are shown in Fig. 8.

As visible in Fig. 8, we find a quite good agreement for conformer A. the peaks are all reproduced within both real-time evolution and Casida TDDFT. The second peak at 6 eV appears only as a shoulder in the real-time evolution spectra. This discrepancy could be reduced increasing the evolution time, since usually the peaks become more sharp when the density can evolve for a longer time.

In order to see if a similar agreement between real-time density-evolution and Casida spectra could be found also at higher convergence, we have calculated σ_x for conformer A using a radius of 8 Å. Comparing σ_x using a radius of 5 Å with that using 8 Å similar differences are observed like in the case of Casida (see Fig. 4) using the same radii. Thus, the spectral changes with respect to the radius are expected to be the same as in Fig. 4.

Nevertheless, the information received from a highly converged real-time density-evolution spectra, which is computationally very demanding, will be the same as from the faster Casida method. For this reason we have not performed this kind of calculations since we cannot expect additional information.

4.5. Discussion of the optical gap

All our calculated spectra show an absorption onset at about 5 eV corresponding to the value of the HOMO-LUMO gap of the system. Such a large gap is quite usual for compounds with a C=C double bond. Our simulations assumed that the molecule is in vacuum, whereas in experiments usually it is in chloroform solution. However, even in polar solvents (e.g., water, $\epsilon = 78.39$), the inclusion of solution effects in the calculation does not affect the value of the gap significantly and also the absorption spectra is influenced only in part (see, e.g., Ref. [33]). Since chloroform is much less polar than water ($\epsilon = 4.9$), large changes in the spectral shape or in the gap are not expected if solvent effects were included in the calculation.

The only available experimental data concerning optical spectra are the measurements of the optical rotation [6,3]. The experimental values are between 1.9 and 3.5 eV, meaning within the absorption gap. These experimental results are not in contradiction to our calculations, since the optical rotation is obtained in transmission and thus, they have to be in the optical absorption gap. Nevertheless, also above the optical absorption gap, it should be possible to measure the optical rotation. From our absorption spectra we can now also predict at which energies in the absorption range of 3-tert-butylcyclohexene the experimental detection of the optical rotation might be successful (here the range up to 6 eV), since absorption and transmission are directly connected.

5. Summary and conclusion

We have presented an ab-initio investigation of the optical spectra of 3-tert-butylcyclohexene. The ground-state structural parameters of the two conformers are in agreement with available reference data. We have investigated the absorption spectra, in particular the photoabsorption cross section for the two conformers of 3-tert-butylcyclohexene based on DFT-IPA and TDDFT. Within the DFT-IPA we have employed the LDA and the GGA approximation where we have found only small differences in the results. For the two conformers the spectra are slightly different. An analysis of the peaks shows that the spectra are mainly determined by transitions from the HOMO to various unoccupied states. For the TDDFT calculation we first utilized the Casida approach. The spectral structure show some similarities comparing DFT-IPA and TDDFT-Casida, but also significant differences: in comparison to the DFT-IPA results, the oscillator strength are shifted to higher energies, mainly due to local field effects. Furthermore, due to the neglect of the mixing of states in the DFT-IPA spectra some peaks appear as split. Thus, a transfer of the interpretation of the spectra from DFT-IPA to TDDFT-Casida or time-evolution TDDFT is difficult. Nevertheless, an analysis of the peaks of the Casida spectra yields a similar interpretation as in the DFT-IPA case. The spectra based on the Casida approach show also differences between the conformers. In particular, a difference in the energy range between 7 and 8 eV can be traced back to a significant influence of the z component of the dielectric function reflecting the main difference between the two conformers: the opposite buckling of the cyclohexene ring. An application of the real-time density-evolution TDDFT did not give significant different spectra compared to the Casida TDDFT ones. Thus, the computational less demanding Casida approach yields reliable results where the spectra can also be interpreted inspecting the corresponding transitions. Since the two conformers are distinguishable by absorption spectra or using anisotropy spectroscopy, we hope that our results will encourage further experimental measurements.

Acknowledgements

This work was partially funded by the EU's 6th Framework Programme through the NANOQUANTA Network of Excellence (NMP4-CT-2004-500198). Computer facilities at CINECA granted by INFM (Project no. 741/2007) are gratefully acknowledged. KGN also wants to thank Elena Cannuccia, Adriano Mosca Conte, Christoph Freysold, Silvana Botti, and Daniele Varsano for fruitful discussions. The authors want to thank especially Rodolfo Del Sole for many useful hints and discussions.

References

[1] G. Bellucci, G. Berti, M. Ferretti, G. Ingrosso, E. Mastrorilli, J. Org. Chem. 43 (1978) 422.
[2] R. Viani, J. Lapasset, J.-P. Aycard, H. Bodot, J. Org. Chem. 44 (1979) 899.
[3] S.K. Sadozai, J.A. Lepoivre, R.A. Dommisse, F.C. Alderweireldt, Bull. Soc. Chim. Belg. 89 (1980) 637.
[4] G. Bellucci, G. Berti, G. Ingrosso, E. Mastrorilli, J. Org. Chem. 45 (1980) 299.
[5] S. Cauwberghs, P.J.D.C.B. Tinant, J.P. Declercq, Tetrahedron Lett. 29 (1988) 2493.
[6] G. Bellucci, G. Ingrosso, A. Marsili, E. Mastrorilli, I. Morelli, J. Org. Chem. 42 (1977) 1079.
[7] D.M. McCann, P.J. Stephens, J. Org. Chem. 71 (2006) 6074.
[8] E. Runge, E.K.U. Gross, Phys. Rev. Lett. 52 (1984) 997.
[9] G. Onida, L. Reining, A. Rubio, Rev. Mod. Phys. 74 (2002) 601.
[10] P. Hohenberg, W. Kohn, Phys. Rev. B 136 (1964) 864.
[11] D.M. Ceperley, B.J. Alder, Phys. Rev. Lett. 45 (1980) 566.
[12] J.P. Perdew, A. Zunger, Phys. Rev. B 23 (1981) 5048.
[13] A.D. Becke, Phys. Rev. A 38 (1988) 2098.
[14] C. Lee, W. Yang, R.G. Parr, Phys. Rev. B 37 (1988) 785.
[15] http://www.pwscf.org.
[16] http://www.tddft.org.
[17] W. Kohn, L.J. Sham, Phys. Rev. A 140 (1965) 1133.
[18] N. Troullier, J.L. Martins, Phys. Rev. B 43 (1991) 1993.
[19] U. von Barth, R. Car, unpublished.
[20] A. DalCorso, S. Baroni, R. Resta, S. de Gironcoli, Phys. Rev. B 47 (1993) 3588.
[21] M.A.L. Marques, A. Castro, G.F. Bertsch, A. Rubio, Comput. Phys. Commun. 151 (2003) 60.
[22] A. Castro, H. Appel, M. Oliveira, C. Rozzi, X. Andrade, F. Lorenzen, M. Marques, E. Gross, A. Rubio, Phys. Stat. Sol. B 243 (2006) 2465.
[23] H. Ehrenreich, M.H. Cohen, Phys. Rev. 115 (1959) 786.
[24] G.F. Bassani, in: Electronic States Optical Transitions in Solids, Pergamon Press, Oxford, 1975, p. 149.
[25] M.A.L. Marques, E.K.U. Gross, in: C. Fiolhais, F. Nogueira, M.A.L. Marques (Eds.), A Primer in Density-Functional Theory, in: Lecture Notes in Physics, vol. 620, Springer, Berlin, 2003, p. 144.
[26] M.A.L. Marques, E.K.U. Gross, Annu. Rev. Phys. Chem. 55 (2004) 427.
[27] M.E. Casida, K.C. Casida, D.R. Salahub, Int. J. Quant. Chem. 70 (1998) 933.
[28] M.E. Casida, C. Jamorski, K.C. Casida, D.R. Salahub, J. Chem. Phys. 108 (1998) 4439.
[29] C. Jamorski, M.E. Casida, D.R. Salahub, J. Chem. Phys. 104 (1996) 5134.
[30] M.E. Casida, T.A. Wesolowski, Int. J. Quant. Chem. 96 (2004) 577.
[31] I. Vasiliev, S. Ögut, J.R. Chelikowsky, Phys. Rev. Lett. 82 (1999) 1919.
[32] K. Yabana, G.F. Bertsch, Phys. Rev. A 60 (1999) 1271.
[33] Y.-K. Choe, S. Nagase, K. Nishimoto, J. Comput. Chem. 28 (2007) 727.